J Solid State Electrochem (2004) 8: 786–793
DOI 10.1007/s10008-004-0546-5

ORIGINAL PAPER

F. Huet · M. Musiani · R. P. Nogueira

Oxygen evolution on electrodes of different roughness: an electrochemical noise study

Received: 12 March 2004 / Accepted: 7 April 2004 / Published online: 9 July 2004

Abstract Rough and porous Ni layers have been obtained by cathodic deposition from a $NiCl_2$, NH_4Cl solution, at high current density. Characterisation by SEM has shown that they consisted of micro-dendrites separated by pores with a typical diameter of 1 μm. In addition, circular hollows (10–100 μm in diameter) were found on the deposit surface; their density varied with the deposition current density and deposition charge. The surface roughness of the Ni deposits, measured by EIS, was found to increase roughly linearly with the deposition charge, and to be little dependent on current density, provided a threshold value was exceeded. The oxygen evolution reaction has been studied on these electrodes by simultaneous real-time measurements of potential and electrolyte resistance fluctuations. The analysis of the electrochemical noise indicated that the dimensions of oxygen bubbles detaching from the electrodes slightly increased with the deposit surface roughness. It is not clear, however, whether or not this increase was associated with the effect of the small (1 μm) or the large (10–100 μm) features on the electrode-bubble interactions.

Keywords Electrodeposition · Impedance · Oxygen · Nickel · Surface roughness · Electrochemical noise

Introduction

Efficient catalysis of electrochemical processes is achieved when both the electronic and the geometric properties of the electrode materials are optimised [1]. While electronic properties are linked to the electrode chemical composition, favourable morphologies are associated with a large surface roughness (that is a large ratio between the effective and the geometric area of the electrode). Of course, an increase in the surface roughness is most beneficial for electrocatalysis when the whole electrode surface is accessible to reactants. This is seldom the case when the reaction products are gases, as bubble formation may considerably reduce the wet area of the electrode by blocking its cavities and pores in a more or less permanent way [2]. Furthermore, the formation of bubbles, their growth on the electrode surface, and their detachment may have a major influence on the cell overpotential by locally enhancing the mass transfer rate and by increasing the electrolyte resistance, both in the solution bulk and near the electrode surface [3, 4].

The nucleation, growth and detachment of bubbles have been thoroughly investigated, and the nature of the electrode material [5, 6] and current density [5, 7, 8] have been found to have major influences on these processes. To the best of our knowledge, little effort has been devoted to ascertaining the effect of surface roughness on the life cycle of electrolytic bubbles. Therefore, in the present study, gas evolution reactions on electrodes of well-defined roughness/porosity have been investigated by electrochemical noise techniques. In particular, oxygen evolution has been studied on porous Ni electrodeposits obtained according to methods recently described in the literature by Marozzi and Chialvo [9, 10].

The present study is based on simultaneous real-time measurements of potential and electrolyte resistance fluctuations, with a device designed with the aim of separating the ohmic and kinetic contributions in the overall potential fluctuations [11]. Theoretical analysis of the experimental results is performed according to a model developed by Gabrielli et al [12, 13] in which the random signal measuring the electrolyte-resistance fluctuations is modelled by a renewal point process. Under certain conditions, this probabilistic approach allows important physical quantities describing the gas

F. Huet · R. P. Nogueira
UPR15-CNRS "Interfaces et Systèmes Electrochimiques",
Université Pierre et Marie Curie, 4 Place Jussieu,
75252 Paris Cedex 05, France

M. Musiani (✉)
CNR-IENI, Corso Stati Uniti 4,
35127 Padova, Italy
E-mail: m.musiani@ieni.cnr.it
Tel.: +39-049-82958866
Fax: +39-049-8295853

evolution process, mainly the mean rate and the mean radius of the detaching bubbles, to be calculated.

Experimental

All chemicals and materials were commercially available. Solutions were prepared with water deionised by a Millipore Milli-RO system. Ni and Ti disc electrodes (0.5 and 0.635 cm in diameter respectively) were made with high purity rods (Goodfellow, 99.99%) the lateral surface of which was protected with a polyacrylate paint. Such an electrode geometry, which avoids the presence of a hydrophobic material surrounding the disc electrode, has proved appropriate in our experiments to prevent sticking of large gas bubbles on the electrode edge, a drawback commonly observed with poly-tetrafluoroethylene sheathed electrodes [14]. Before Ni deposition, the Ni and Ti electrodes were polished with emery paper, then alumina (0.3 μm) and rinsed with water. The Ti electrodes were further etched in 5% HF for 10 s, rinsed again and dried in an air stream.

The Ni porous electrodes used in this study were obtained by Ni^{2+} reduction. Ni was electrodeposited, according to Marozzi and Chialvo [9, 10], from a 0.2 M $NiCl_2 + 2$ M NH_4Cl solution, at large current density (up to -2 A cm^{-2}) in a compartmented cell [15] using Ni or Ti rotating discs as working electrodes and a Pt grid as counter electrode. The surface roughness of the electrode was controlled by varying either the deposition current density j, or the deposition charge jt, where t is the deposition time. The Ni electrodeposits were rinsed with deionised water and dried in an air stream before the electrochemical impedance spectroscopy (EIS) and electrochemical noise measurements.

EIS experiments, aimed at establishing the surface roughness of the Ni electrodes, were carried out with a Solartron 1254 Frequency Response Analyser and a 1286 Electrochemical Interface, driven by a commercial software (Fracom by P. Bernard and H. Takenouti). The impedance was measured in 1 M $NaNO_3$, at the open circuit potential.

Electrochemical noise experiments on horizontal electrodes facing upwards were carried out galvanostatically. Oxygen evolution was studied in a 1 M NaOH solution at room temperature, mainly at anodic current densities of 25 mA cm^{-2}. Potential and electrolyte resistance fluctuations were measured simultaneously after at least one hour of prepolarization in order to ensure steady-state conditions. The time records were acquired with a real-time computer (Concurrent Computer RTU 5450), which also calculated their power spectral densities (PSDs) by means of the periodogram method using the fast Fourier transform [16]. Several sampling rates were successively used to enlarge the analysed frequency range. To increase the PSD accuracy, ten time records were acquired at each sampling rate, and the PSDs calculated for each time record were averaged.

Results and discussion

Preparation of Ni electrodes

Ni electrodes were prepared by electrodepositing Ni from a 0.2 M $NiCl_2 + 2$ M NH_4Cl solution, according to Marozzi and Chialvo [9, 10]. These authors claimed that very rough and mechanically stable deposits may be obtained at large current densities in the presence of ammonium chloride. Our experiments fully confirmed their report. In their work, Marozzi and Chialvo studied the dependence of surface roughness on deposition current density. As they prepared all samples with the same deposition time (1 h), the deposition charge varied along with the current density. Furthermore, they showed that the current efficiency of Ni deposition somewhat decreased with increasing current. Therefore, in order to assess the influence of each variable on electrode roughness, we investigated the respective roles of current density, deposition charge and deposit thickness.

The current efficiency of Ni deposition was derived from charge and weight measurements. Figure 1 shows the influence of the current density on the current efficiency averaged on five samples prepared with deposition charges in the range 100–500 C cm^{-2} (the charge had a very small influence on current efficiency). The smooth decrease shown in Fig. 1 agrees with the results of Marozzi and Chialvo, although our efficiency values are generally lower than theirs [9]. The use of a facing-down electrode, rotating at a high angular speed (2500 rev min^{-1}) may be the reason for such a difference.

Characterisation of Ni deposits by EIS

In order to measure the surface roughness, we recorded impedance spectra at the open circuit potential in an

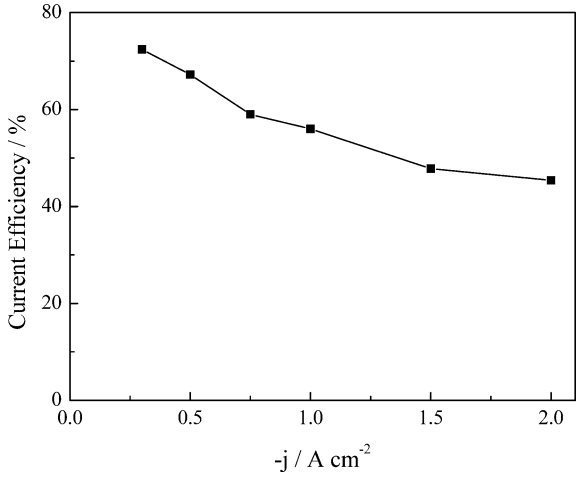

Fig. 1 Dependence of the average current efficiency of Ni deposition on current density. The average was calculated for five samples prepared with deposition charges in the range 100–500 C cm^{-2}

inert electrolyte. This method, already used in [17], yields the surface roughness as the ratio of the double-layer capacitances of a rough and an ideally smooth electrode of the same nature. It is well-established that the double layer capacitance of rough or porous electrodes must be measured at a frequency low enough for the penetration depth of the AC signal to be equal to the pore length [18, 19, 20, 21, 22, 23, 24, 25, 26, 27], so that the whole inner surface of the pores is sampled. Figure 2 compares the Nyquist plots obtained with a Ni disc polished with 0.3 μm alumina, assumed to be ideally flat (empty dots) and a rough Ni electrodeposit (full symbols). Two major differences are observed: (i) a straight line forming an angle of ~45° with the real axis is seen at high frequency only for the electrodeposit, as expected for a rough or porous electrode [18, 19, 20, 21, 22, 23, 24, 25, 26, 27], and (ii) the capacitive behaviour is shifted to much lower frequency in the case of the electrodeposit, testifying its much larger capacitance.

Figure 3 shows the dependence of surface roughness on deposition charge, measured on samples prepared with the same current density ($j = -2$ A cm^{-2}). It is clear that the deposition charge has a major influence. As a first approximation, a linear dependence of surface roughness on deposition charge may be assumed, the deviations being possibly due to outgrowth of the deposit beyond the disc edge (increase in geometric area) at the larger deposition charges. In other words, the surface roughness of deposits prepared at the same current density can be considered as linearly dependent on the deposit thickness.

Figure 4 shows the effect of j on surface roughness. If samples obtained with the same deposition charge are compared, a well-defined maximum is visible (empty dots). If one takes into account the decrease in current efficiency with increasing j (see Fig. 1), and prepares samples of constant deposit weight, the current density-surface roughness curve still exhibits a maximum, but not a marked one (filled dots).

The data reported in Figs. 3 and 4 reveal that the dependence of surface roughness on the experimental variables is more involved than that described by Marozzi and Chialvo [9, 10] who reported that the surface roughness depends linearly on j, which meant a linear dependence on deposition charge under their experimental conditions. Our data show that a significant roughness is observed only when j exceeds a threshold (not described by Marozzi and Chialvo) after which the roughness becomes almost independent of j for samples prepared with constant deposit weight (constant thick-

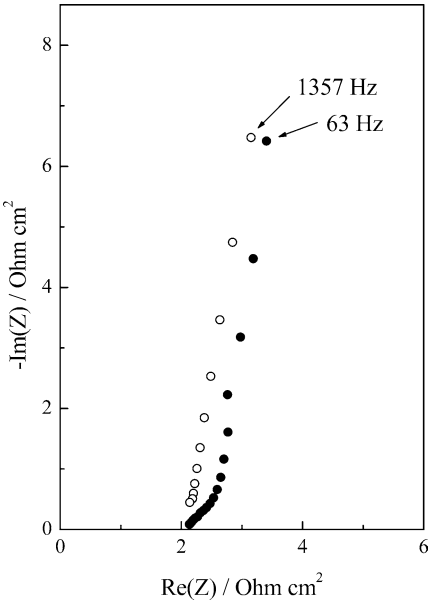

Fig. 2 Nyquist plots of the impedance of a Ni electrode polished with alumina (empty dots) and a Ni electrodeposit (filled dots) recorded in 1 M $NaNO_3$ at the open circuit potential. Deposition was carried out in 0.2 M $NiCl_2 + 2$ M NH_4Cl solution, at a current density of -2 A cm^{-2}, with a deposition charge of 100 C cm^{-2}

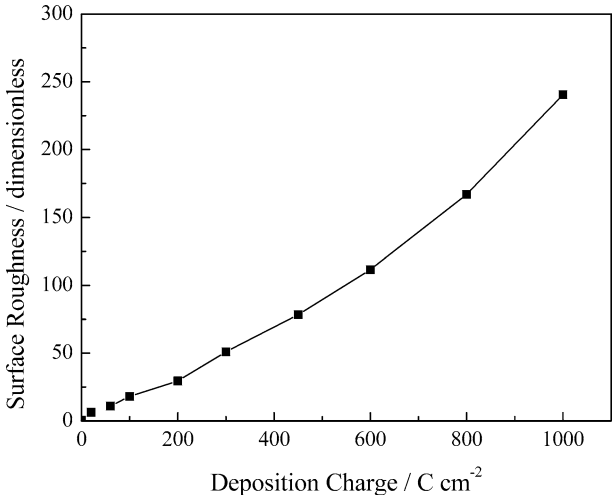

Fig. 3 Dependence of surface roughness on deposition charge for Ni electrodes deposited from a 0.2 M $NiCl_2 + 2$ M NH_4Cl solution at a current density of -2 A cm^{-2}

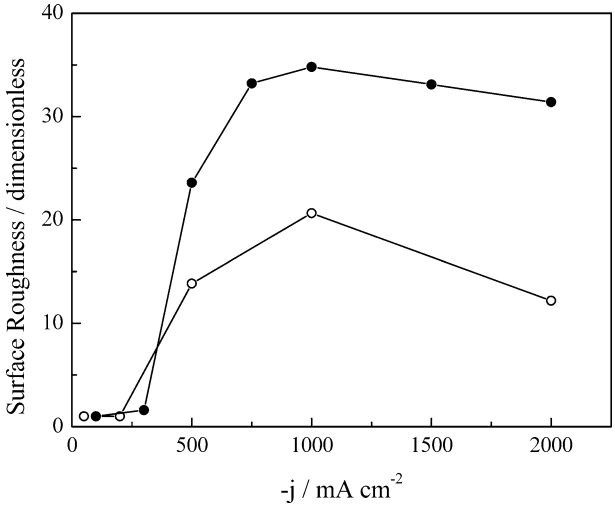

Fig. 4 Dependence of surface roughness on Ni deposition current density. Empty dots correspond to deposits obtained with a constant deposition charge (200 C cm^{-2}), filled dots to deposits of constant mass (50 mg cm^{-2})

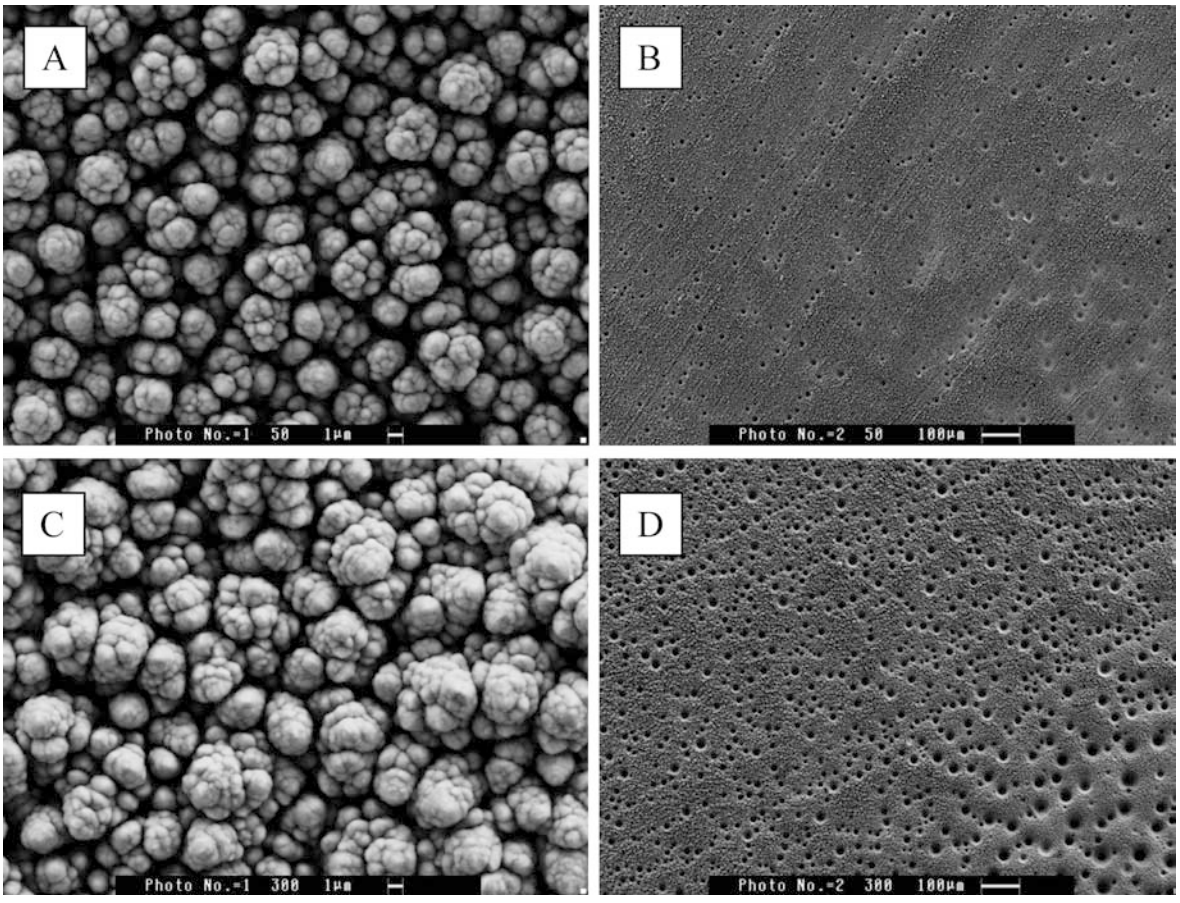

Fig. 5 SEM images of Ni deposits obtained at -1 A cm^{-2} with different deposition charges: A and B: 50 C cm^{-2}; C and D: 300 C cm^{-2}

ness). In this range of large deposition currents, the surface roughness varies quasi-linearly with the deposition charge (that is with the deposit thickness), as observed in Fig. 3.

Characterisation of Ni deposits by SEM

Ni deposits obtained at various current densities (and constant thickness), or obtained with different deposition charges (and constant current density) were submitted to SEM analyses. The effect of deposition charge is shown in Fig. 5. At large magnification (A and C), both deposits appear micro-dendritic: at both deposition charges one observes crystallites of comparable size. The linear dependence of the effective electrode area on the deposition charge, shown by EIS experiments, suggests that the pores (the lateral dimensions of which are essentially independent of deposition charge) have a depth comparable to the deposit thickness. At lower magnification (B and D) an additional feature becomes evident: circular hollows, 10–40 μm in diameter, are present in both samples, but their number substantially increases with deposition charge (deposition time). Additional samples, not shown here, confirm that the density of hollows varies with deposition charge in a continuous, monotonic way. These hollows are interpreted as the result of hydrogen bubbles, formed in a parasitic process during Ni deposition, and residing on the electrode surface, despite the forced convection, for a time long enough to locally hinder Ni deposition.

The effect of deposition current density is shown in Fig. 6. The diameters of the hollows decreased markedly while their density increased markedly as the deposition current density increased. At greater magnification, not shown here, all samples appear to consist of micro-dendrites of comparable size.

On the basis of this SEM investigation, the roughness of Ni deposits is shown to be the result of features of two different characteristic sizes: deep pores not much wider than 1 μm and shallow hollows with diameters in the range 10–100 μm. The surface roughness measured by EIS is expected to take into account both features, without possible discrimination between them. After the electrochemical noise study reported in the following section, the Ni electrodes were again submitted to SEM and found to have retained their initial morphology.

Electrochemical noise characterisation of oxygen evolution

The Ni deposits submitted to electrochemical noise measurements were prepared with the same current

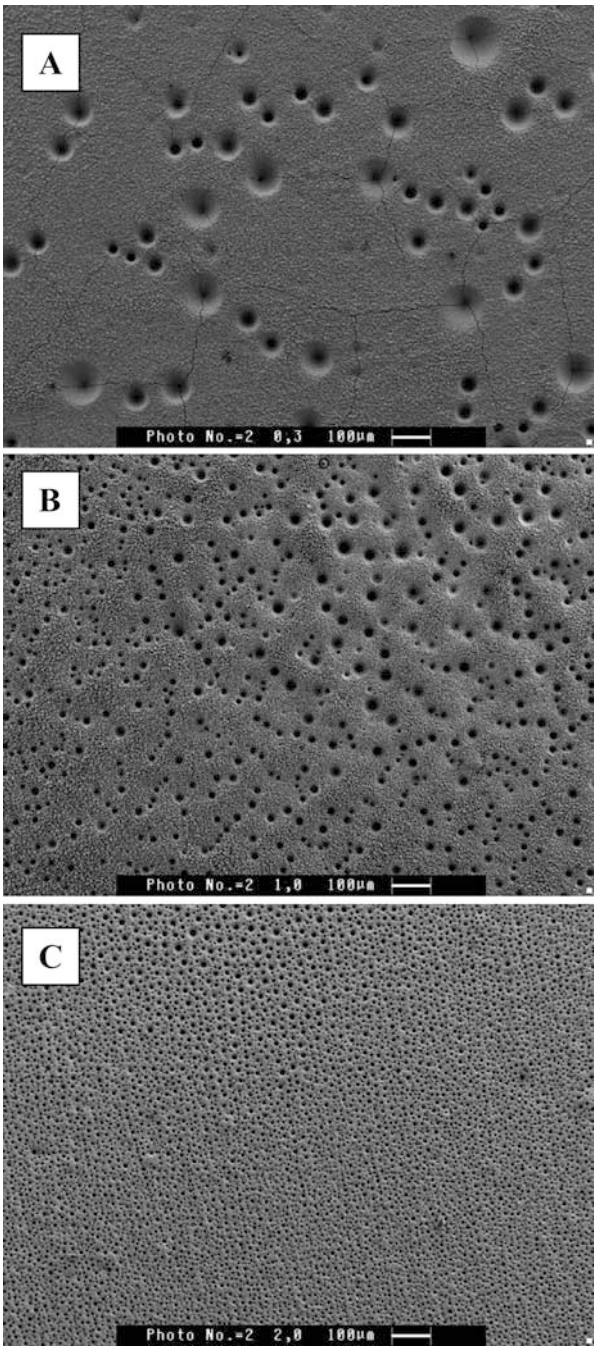

Fig. 6 SEM images of Ni deposits obtained with a current density of −0.3 (A), −1 (B), and −2 A cm^{-2} (C). For all samples the Ni deposit mass was 50 mg cm^{-2}

density (−2 A cm^{-2}) and variable deposition charge, as the latter experimental parameter is the one influencing the surface roughness in a simpler way. The deposition charge was varied between 10–160 C cm^{-2}; therefore, according to Fig. 3, the samples had a surface roughness between 1.5 and 24 (the surface roughness of Ni polished with 0.3 µm alumina was conventionally assumed to be 1). Ni layers prepared with larger deposition charges were not investigated, since their adhesion to the substrates (especially Ti) was not fully satisfactory during prolonged electrolyses, perhaps because of hydrogen embrittlement during deposition at strong cathodic current densities.

A first important remark about the electrochemical noise results concerns the current density range applied in the galvanostatic control of the interface. Preliminary measurements showed that low current density values did not yield steady-state responses. Indeed, at current density values lower than 10 mA cm^{-2}, even if the electrode geometry described above strongly prevented the presence of big oxygen bubbles sticking at the edge of the electrode, this border region remained prone to trapping bubbles anchored on it for a long time. As a consequence, the few edge bubbles still present showed a very slow life cycle, causing the potential and electrolyte resistance signals to drift. Therefore, the electrochemical noise analysis has been mainly performed in an intermediate current density range of oxygen evolution, typically $j = 25$ mA cm^{-2}. Under these conditions, the overall potential fluctuations measured for the different roughness values investigated in this study were governed by purely ohmic effects induced by dynamic bubble evolution on the electrode surface. Figure 7 illustrates, as an example, the behaviour of a Ni electrode with a surface roughness of 3. It can be seen that the PSD of the potential fluctuations, Ψ_V, is almost perfectly coincident with the ohmic-drop fluctuations PSD, Ψ_{ReI}, derived from the PSD of the electrolyte resistance fluctuations, Ψ_{Re} ($\Psi_{ReI} = I^2\Psi_{Re}$). This means that, at intermediate current density values, the bubble evolution clearly controls the stochastic behaviour of the interface and that both potential and electrolyte resistance noises convey the same information, as is clearly shown in Fig. 7. This is why the results presented hereafter concern the electrolyte resistance fluctuations only, since they allow a straightforward and more intuitive approach to bubble evolution phenomena.

The electrolyte resistance noise obtained at $j = 25$ mA cm^{-2} varies slightly but significantly with the surface roughness. Figure 8 shows the Ψ_{Re} plots

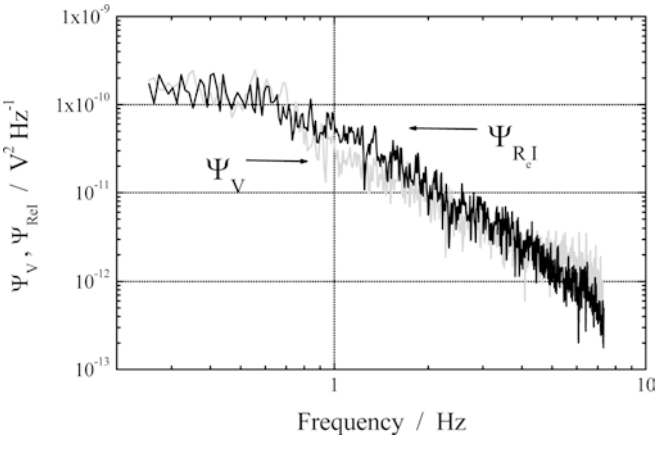

Fig. 7 PSD of potential, Ψ_V, and ohmic-drop fluctuations, Ψ_{ReI}, measured at 25 mA cm^{-2} for an electrode with a surface roughness of 3

obtained for electrodes with surface roughnesses of 3 and 24. The PSDs obtained for intermediate values of surface roughness have not been plotted for the sake of clarity, as they all fall between these limiting curves. However, it is interesting to note that even if the maximum amplitude shift was only approximately half a decade, as shown in Fig. 8, there was a slight monotonic increase in the PSD amplitude with the surface roughness, as further discussed below.

The general behaviour of Ψ_{Re} expected for the ensemble of the electrodes consists of a low-frequency plateau followed by a $1/f^{\alpha}$ roll-off (where f is the frequency and $\alpha = 2$). This is the frequency-domain representation corresponding to a saw-tooth shape of the time record $Re(t)$ (due to the slow growth and sudden departure of the bubbles) modelled by a renewal point-process, as already discussed elsewhere [13, 28]. Indeed, the expression for the PSD corresponding to such time records is (for a complete discussion on the derivation of this expression and the underlying assumptions, see [28]):

$$\Psi_{Re}(f) = \frac{2\lambda\langle \Delta Re^2 \rangle}{\lambda^2 + 4\pi^2 f^{\alpha}}, \quad \alpha = 2 \tag{1}$$

where λ is the mean bubble detachment rate and $<\Delta Re^2>$ is the average of the squared amplitude of the electrolyte resistance drops caused by bubble departures; λ and $<\Delta Re^2>$ can be obtained from the PSD by:

$$\lambda = 2\pi f_c \tag{2}$$

and

$$\langle \Delta Re^2 \rangle = \pi f_c \Psi_{Re}(0) \tag{3}$$

respectively, where $\Psi_{Re}(0)$ represents the low-frequency plateau and f_c is the cut-off frequency defined as the frequency at which $\Psi_{Re}(f_c) = \Psi_{Re}(0)/2$. Further development of the model leads to the expression of the mean detachment radius $<r_b>$:

$$\langle r_b \rangle = \sqrt{\frac{S}{\pi \alpha_e \langle Re \rangle}} \langle \Delta Re^2 \rangle^{1/4} \tag{4}$$

where S is the geometric electrode surface area, $<Re>$ is the mean Re value and α_e is a dimensionless coefficient determined empirically ($\alpha_e \approx 0.4$) [28].

In spite of some variation in the roll-off slope ($2 < \alpha < 2.4$), Eqs. 1–4 allowed us to simulate the experimental PSDs and to estimate the mean size of the detaching bubbles, which depends mainly on the low-frequency plateau level $\Psi_{Re}(0)$ and on the cut-off frequency f_c (see Eqs. 3 and 4). Figure 9A illustrates the good agreement between the measured PSD and that simulated with Eq. 1 for the electrode with a surface roughness of 6, as an example, whilst Fig. 9B presents the simulated PSDs for all electrodes (roughnesses between 3 and 24), confirming a slight but definite monotonic increase in the PSD amplitude with the surface roughness. In contrast, no significant change in the cut-off frequency may be observed, all PSDs being nearly "parallel", which indicates that the bubble detachment rate was independent of the electrode surface roughness. The bubble departure mean radii were estimated from the simulated curves in Fig. 9B and Eq. 4. The resulting values given in Fig. 10 show a slight increase with the surface roughness. It is important to stress that the estimated bubble diameters (≥200 μm) are

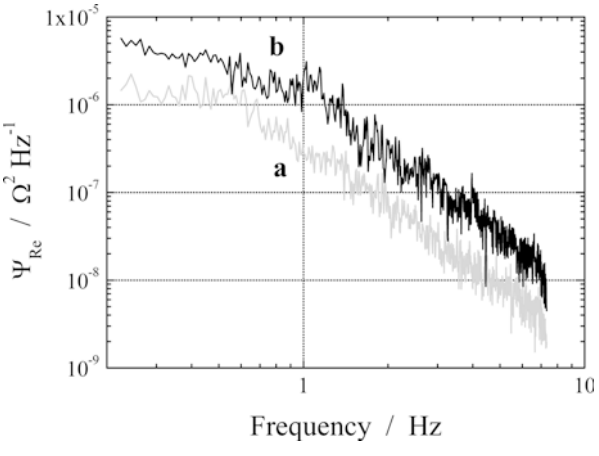

Fig. 8 PSD of electrolyte resistance fluctuations, Ψ_{Re}, measured at 25 mA cm^{-2} for an electrode with a surface roughness of 3 (curve a) and 24 (curve b)

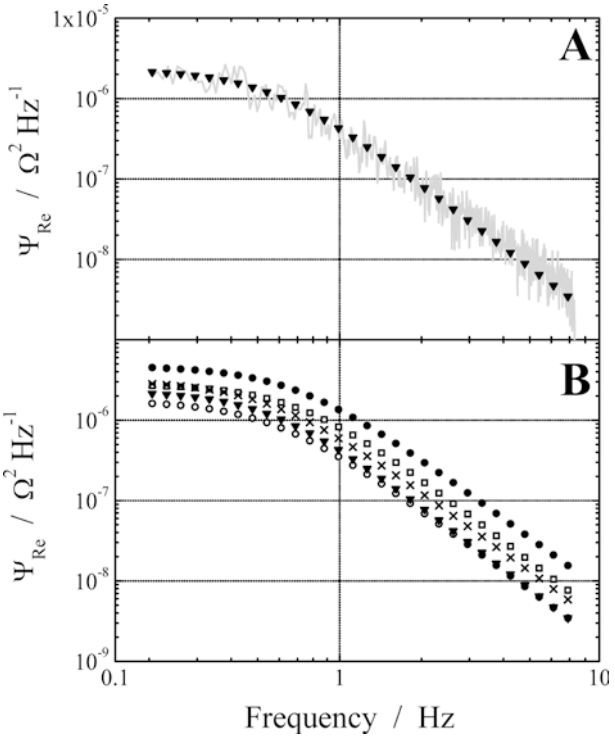

Fig. 9 (A) Measured and simulated PSDs of electrolyte resistance fluctuations, Ψ_{Re}, measured at 25 mA cm^{-2} for an electrode with surface roughness of 6. (B) Simulated Ψ_{Re} for a surface roughness of 3 (empty circles); 6 (triangles); 12 (crosses); 18 (squares); 24 (filled circles)

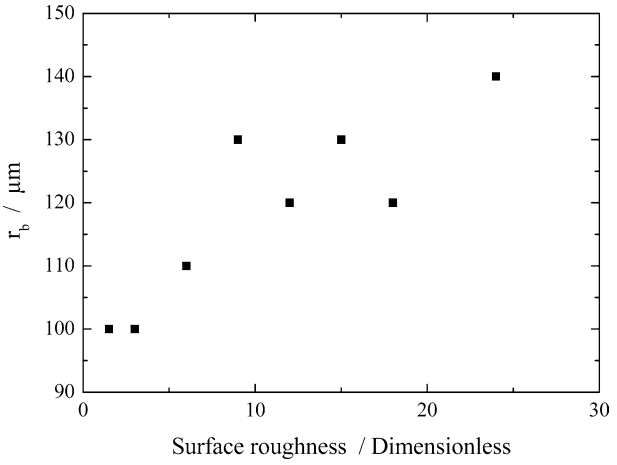

Fig. 10 Bubble departure mean radius calculated from Eq. 4 for different surface roughness values

much larger than most of the roughness features seen in Figs. 5 and 6C (typically a few μm); they are rather in the dimension range of the fairly rare large hollows present on the surface. This indicates that, at least in the roughness range investigated (from 3 to 24), there is no direct relationship between the mean size of the bubbles and that of the surface irregularities, as there should be if each bubble evolved on a small surface cavity or irregularity.

The interpretation of the observed increase in the bubble detachment radius, and hence of the slight intensification of the electrolyte resistance noise, is not straightforward. In fact, bubble evolution on rough surfaces is a very complex phenomenon. From a purely geometric point of view, rougher electrodes offer a larger effective area for reactions to take place and a consequent lower local current density that could proportionally decrease the concentration in dissolved oxygen and then hinder gas evolution. On the other hand, a higher density of surface irregularities could act either as active sites that are physically favourable for heterogeneous bubble nucleation (and therefore decrease the oxygen saturation threshold necessary to trigger bubble evolution) or as gas cavities that locally accumulate dissolved oxygen and favour the achievement of the critical concentration [29, 30], also favouring bubble evolution. The balance between these opposite effects may effectively lead to a certain dependence of the bubble evolution features on the surface roughness, as found in this study, but strikingly large differences in the dynamic bubbling regime for electrodes of the same material submitted to the same overpotential should not be expected. Furthermore, as the relative weight of these opposite effects cannot be estimated, it is not possible to predict a priori whether an increase in surface roughness will lead to increasing or decreasing $< r_b >$ values.

Further electrochemical noise experiments were carried out at larger current density values ($j > 100$ mA cm^{-2}). Under these conditions of very strong bubble evolution, the PSD curves obtained on electrodes of various roughnesses almost perfectly overlapped, which provided no clear indication of a possible effect of surface roughness on bubble evolution regime.

Conclusions

Nickel electrodes obtained by cathodic deposition from nickel chloride, ammonium chloride solutions at large current density are extremely porous. Their surface roughness is due both to "small" (micro-dendrites separated by deep pores of typically 1 μm diameter) and "large" (circular hollows with 10–100 μm diameters) features, the former being much more numerous than the latter, and therefore accounting for most of the developed area of these electrodes. Both deposition current density and deposition charge influence each type of feature, but the surface roughness depends primarily on deposition charge, when j is above a critical threshold. When O_2 is anodically evolved on these electrodes at intermediate current density ($10 < j < 100$ mA cm^{-2}), the potential and electrolyte resistance noise level monotonically increases for increasing surface roughness, as a result of an increase in the mean detachment radius of the bubbles. The available experimental results do not evidence any relationship between the size of the detaching bubbles and the presence of "small" or "large" features. This aspect will be further investigated by studying electrodes with a monodisperse pore dimension.

Acknowledgements The authors thankfully acknowledge the experimental assistance of Mr. Stephan Borensztajn who recorded SEM images.

References

1. Trasatti S (2000) Electrochim Acta 45:2377
2. Lohrberg K, Khol P (1984) Electrochim Acta 29:1557
3. Vogt H (1983) In: Yeager E, Bockris JOM, Conway BE, Sarangapani S (eds) Comprehensive treatise of electrochemistry, vol 6: electrodics: transport. Plenum, New York, p 445
4. Sides PJ (1986) In: White RE, Bockris JOM, Conway BE (eds) Modern aspects of electrochemistry, Vol 18. Plenum, New York, p 303
5. Venczel J (1970) Electrochim Acta 15:1909
6. Ibl N, Venczel J (1970) Metalloberfläche 24:365
7. Janssen LJJ, Hoogland JG (1973) Electrochim Acta 18:543
8. Landolt D, Acosta R, Muller RH, Tobias CW (1970) J Electrochem Soc 117:839
9. Marozzi CA, Chialvo AC (2000) Electrochim Acta 45:2111
10. Marozzi CA, Chialvo AC (2001) Electrochim Acta 45:861
11. Gabrielli C, Huet F, Keddam M (1991) J Electrochem Soc 138:L82
12. Gabrielli C, Huet F, Keddam M, Macias A, Sahar A (1989) J Appl Electrochem 19:617
13. Gabrielli C, Huet F, Keddam M, Sahar A (1989) J Appl Electrochem 19:683
14. Huet F, Nogueira RP, Musiani M (2003) Electrochim Acta 48:3981
15. Musiani M, Furlanetto F, Guerriero P (1997) J Electroanal Chem 440:31

16. Bertocci U, Frydman J, Gabrielli C, Huet F, Keddam M (1998) J Electrochem Soc 145:2780
17. Casellato U, Cattarin S, Musiani M (2003) Electrochim Acta 48:3991
18. De Levie R (1963) Electrochim Acta 8:751
19. De Levie R (1964) Electrochim Acta 9:1231
20. De Levie R (1965) Electrochim Acta 10:113
21. De Levie R (1967) In: Delahay P (ed) Advances in electrochemistry and electrochemical engineering, Vol VI. Wiley, New York, p 329
22. Keiser H, Boccu KD, Gutjahr MA (1976) Electrochim Acta 21:539
23. Candy JP, Fouilloux P, Keddam M, Takenouti H (1981) Electrochim Acta 26:1029
24. Candy JP, Fouilloux P, Keddam M, Takenouti H (1982) Electrochim Acta 27:1585
25. Eloot K, Debuyck F, Moors M, Van Peteghem AP (1995) J Appl Electrochem 25:326
26. Eloot K, Debuyck F, Moors M, Van Peteghem AP (1995) J Appl Electrochem 25:334
27. Song HK, Jung YH, Lee KH, Dao LH (1999) Electrochim Acta 44:3513
28. Silva JM, Nogueira RP, Miranda L, Huet F (2001) J Electrochem Soc 148:E241
29. Jones SF, Evans GM, Galvin KP (1999) Adv Colloid Interface Sci 80:27
30. Jones SF, Evans GM, Galvin KP (1999) Adv Colloid Interface Sci 80:51